REALIZATION CALCULUS

Finite Resolution

A visual atlas

Coupled functions, exact recovery
and the limits of observation

Komorebi P.

How to use this atlas

This atlas develops three quantitative examples of finite resolution and a family of two interacting entire functions. Fourteen computed plates connect the definitions, parameter geometry, growth laws, precision certificates and exact recovery. Complete proofs appear in the accompanying *Special Functions* monograph.

An exact rational inequality is a certificate. A numerical curve illustrates its scale within its stated truncation and precision. Neither replaces the analytic proof of a statement about an infinite object. The limits of each construction are recorded alongside its results.

Contents

How to use this atlas i

Coupled growth and the cost of resolution 1

A small change can alter the global order 2

How far is far enough to guarantee separation? 3

A large excluded prime hides in a fixed window 4

Seeing the prime can make subtraction harder 5

A degree-seven witness exposes a signed defect 6

Passing every coarse test can still miss the defect 7

Two functions exchange growth 8

The coefficients preserve both addresses 9

One order, two exact type proportions 10

Growth follows a spectral surface 11

A coefficient list with a certified tail 12

The phase calculus transports the pair 13

Two surfaces where one component rescales to the other 14

Degree seven identifies the four scales 15

What the coupled extension establishes 16

Where the coupled construction sits 17

COUPLED FAMILIES

Coupled growth and the cost of resolution

The coupled family consists of two entire functions whose derivatives depend on contracted values of both components. Its growth exponent is the unique positive number ρ for which

$$\operatorname{spr}\begin{pmatrix} q^{\rho} & r^{\rho} \\ a^{\rho} & b^{\rho} \end{pmatrix} = 1, \qquad 0 < q, r, a, b < 1.$$

Both functions have positive lower type and finite upper type at this order. The positive eigenvector fixes the proportions of both type vectors. The existence of an ordinary type limit remains open.

Local coefficients reveal the coupling

Two explicit parameter surfaces describe exactly when one normalized component is an amplitude and argument rescaling of the other. Outside these surfaces, the coefficients through degree seven recover all four ordered scales. This provides an exact local inverse for the labeled pair.

Three ways finite observations can miss structure

The resolution atlas compares a weak tap, a large excluded prime, and a negative sieve atom. Each example links a structural change to a concrete observation scale and a proved certificate.

Example	Observation	What the certificate gives
Weak feedback tap	Values on a complex disk	An explicit compact error and a sufficient radius for separation
Excluded prime	Values and derivatives	Exact disk bounds and a negative-depth visibility bracket
Negative sieve atom	All polynomial tests up to a degree	Positive squared-polynomial integrals through degree four and a negative degree-seven witness

The computed plates follow in thematic sections. Complete derivations accompany the full monograph, and the source archive contains the alternative growth proof, exact laboratory, and review records. The six-source literature comparison identifies classical antecedents. Historical priority of the specific coupled results remains unresolved.

How to read the figures

An exact rational bound supplies a certificate. A decimal display illustrates its size. Numerical curves retain their stated truncation and precision, and the universal growth and recovery statements rest on their proofs.

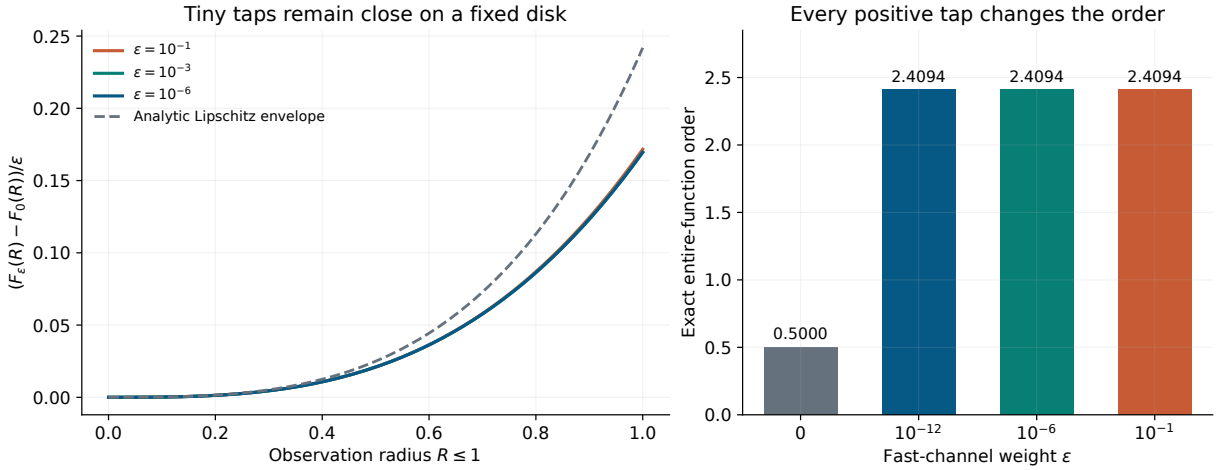
RESOLUTION ATLAS / WEAK TAPS

A small change can alter the global order

A feedback channel may be almost invisible on a fixed disk and still determine the eventual growth of the function. Consider the normalized entire solution

$$F_\varepsilon'(z) = 1 + (1-\varepsilon)F_\varepsilon(z/4)^2 + \varepsilon F_\varepsilon(3z/4)^2, \qquad F_\varepsilon(0) = 0.$$

Here $0 \le \varepsilon \le 1$. At $\varepsilon = 0$, its entire order is $1/2$. At every positive weight, the order becomes $\rho = \log 2/\log(4/3) \approx 2.40942084$.



Left: divide the compact difference by the tap weight to compare its shape. Right: the proved order jumps at zero. The dashed curve is an analytic envelope. The function curves use 100-digit arithmetic and have a normalized omitted-series bound below 5.26×10^{-23} on $0 \le R \le 1$. Floating rounding is separate from that tail bound.

The unit disk comes with an exact error certificate

Let $f_{3/4} = F_1$, with $f_{3/4}(z) = \sum_{n\ge 0} d_n z^{2n+1}$. Positive coefficients give

$$\sup_{|z|\le R} |F_\varepsilon(z) - F_0(z)| \le \varepsilon \sum_{n\ge 1} n d_n R^{2n+1}.$$

A rational coefficient sum and a positive-tail estimate prove that, on the unit disk, the multiplier is less than 0.241890267. For $\varepsilon = 10^{-12}$, the entire disk therefore changes by less than $2.41890267 \times 10^{-13}$.

The observation window and the global invariant answer different questions. Exact measurements can distinguish the functions. With an absolute error allowance at least half the displayed bound, midpoint data can fit both. The order concerns the limit through arbitrarily large radii, where the active faster channel eventually matters.

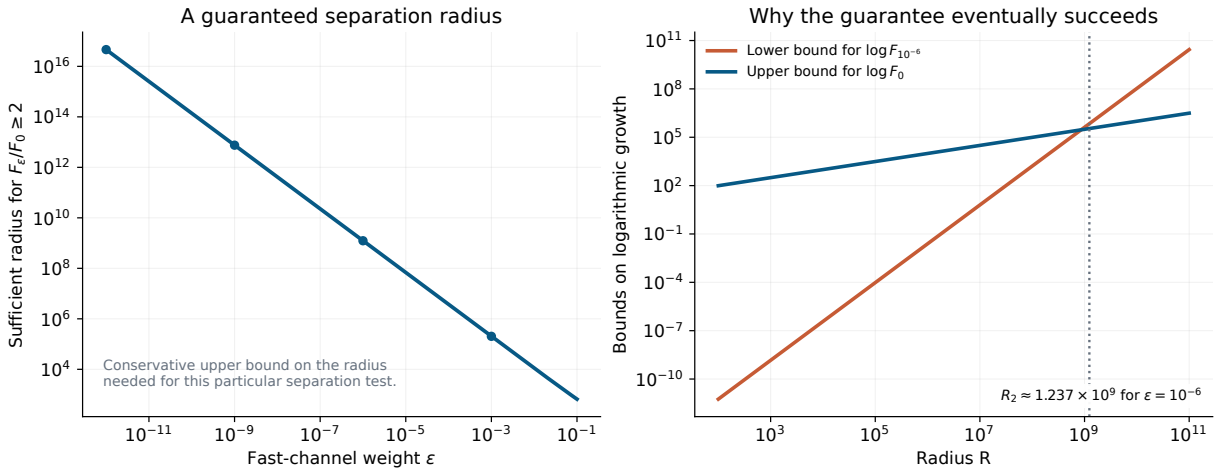
RESOLUTION ATLAS / OBSERVATION RADIUS

How far is far enough to guarantee separation?

The growth theorem supplies positive lower type for the weak-tap function and finite upper type for the slow function. For $0 < \varepsilon \le 1$ and $R \ge e$,

$$\log F_\varepsilon(R) \ge c_\varepsilon R^\rho, \qquad \log F_0(R) \le C_0\sqrt{R},$$

$$c_\varepsilon = \frac{\log 2}{(4/\varepsilon + 8/3)^\rho}, \qquad C_0 = e^{-1/2}(1 + 22\log 2).$$



The left curve is a sufficient radius obtained from conservative comparison constants. The right panel shows why the lower bound for the perturbed function eventually exceeds the upper bound for the slow one. These are bounds on logarithmic growth, rather than numerical evaluations at the large plotted radii.

An explicit sufficient radius

Put

$$R_2(\varepsilon) = \max\left\{ e, \left(\frac{2C_0}{c_\varepsilon}\right)^{1/(\rho-1/2)}, \left(\frac{2\log 2}{c_\varepsilon}\right)^{1/\rho} \right\}.$$

Then $F_\varepsilon(R) \ge 2F_0(R)$ for every $R \ge R_2(\varepsilon)$. The formula makes $c_\varepsilon R^\rho$ at least both $2C_0\sqrt{R}$ and $2\log 2$, and therefore at least their half-sum. Exponentiating gives the factor of two.

For $\varepsilon = 10^{-6}$, the formula is approximately 1.237×10^9. This large radius is a guaranteed sufficient choice. It is not the first radius at which a useful difference appears, and it does not establish failure of every observation at smaller radii. The exact formula carries the guarantee. Rounded figures illustrate its scale.

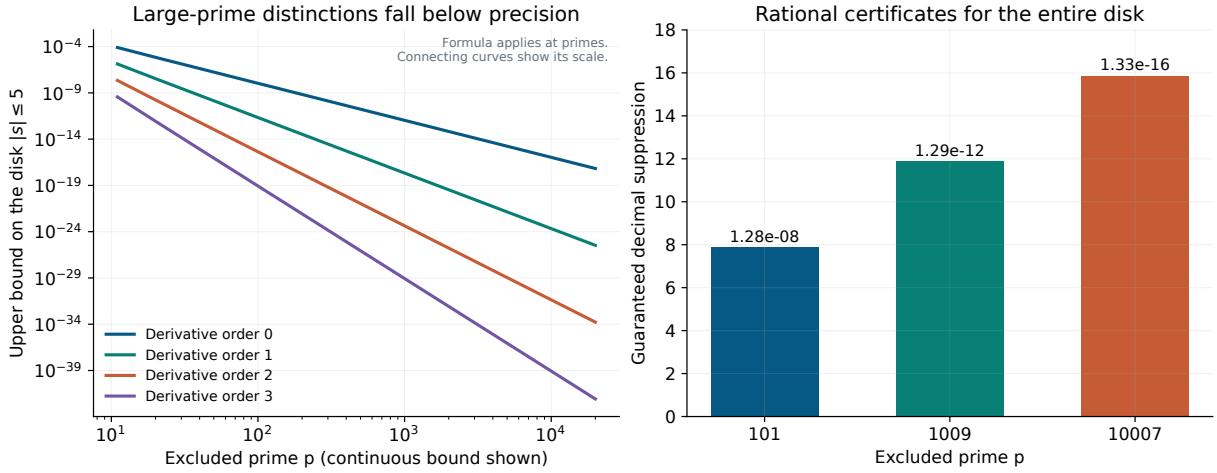
RESOLUTION ATLAS / ARITHMETIC PRECISION

A large excluded prime hides in a fixed window

Use the squarefree arithmetic family

$$A_Q(s) = \sum_{\substack{n\geq 2\\ \mu(n)^2=1\\ (n,Q)=1}} n^{-4}(1-n^{-2})^{2s}, \qquad D_p(s) = A_1(s) - A_p(s),$$

where p is prime. The difference contains exactly the squarefree atoms divisible by p. Its largest frequency is $\lambda_p = -2\log(1-p^{-2})$, and its total mass is $D(4)/(p^4+1)$, with $D(4) = 105/\pi^4$.



Left: analytic bounds for the function and three derivatives on $|s| \leq 5$. The connecting curves show scale, while the arithmetic statement applies at primes. Right: rational bounds for three particular excluded primes. The bar height is the negative base-ten logarithm of the bound, not a count of recovered digits.

The full complex disk has a rational certificate

For integer $k \geq 0$,

$$\sup_{|s|\leq 5} |D_p^{(k)}(s)| < \frac{4(1-p^{-2})^{-10}}{3(p^4+1)} \left(\frac{2}{p^2-1}\right)^k.$$

The inequality uses $D(4) < 4/3$ and $\lambda_p \leq 2/(p^2-1)$. Every quantity on the right is rational. For $k = 0$, upward decimal bounds are 1.283×10^{-8} at $p = 101$, 1.287×10^{-12} at $p = 1009$, and 1.330×10^{-16} at $p = 10007$.

The excluded prime changes the exact inverse of the function. Nevertheless, its effect becomes arbitrarily small on every fixed disk, including in every fixed derivative order. A bounded error model therefore needs an arithmetic parameter bound if it is to promise uniform recovery.

RESOLUTION ATLAS / NEGATIVE DEPTH

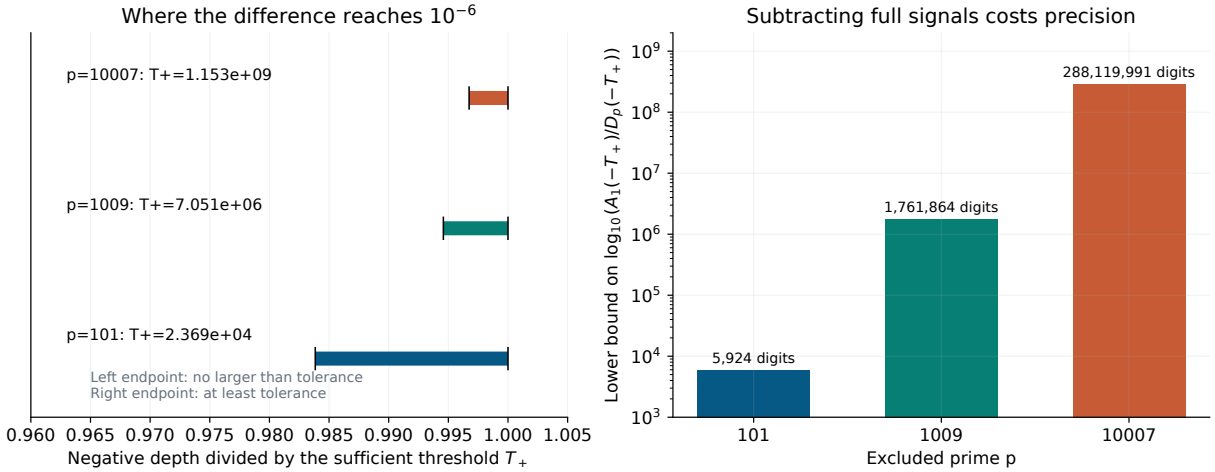
Seeing the prime can make subtraction harder

At negative real depth, the difference grows. The prime atom alone supplies a lower bound, while the entire removed shelf supplies an upper bound:

$$p^{-4}e^{\lambda_p T} \le D_p(-T) \le \frac{D(4)}{p^4+1}e^{\lambda_p T}, \qquad T \ge 0.$$

Choose a tolerance $\eta > D(4)/(p^4+1)$. Its unique crossing occurs between

$$T_- = \frac{\log(\eta(p^4+1)/D(4))}{\lambda_p}, \qquad T_+ = \frac{\log(\eta p^4)}{\lambda_p}.$$



At tolerance 10^{-6}, the left panel shows the analytic crossing brackets after rescaling each row by T_+. The right panel shows a lower bound on the decimal cancellation scale when subtracting full functions. Displayed endpoints and labels are ordinary floating evaluations of exact formulas.

For $p = 101$, the difference is no larger than 10^{-6} through $T_- = 23307.789\ldots$, and at least that large by $T_+ = 23690.516\ldots$. The decimals illustrate the formulas and are not rounded interval certificates.

The direct positive difference and subtraction have different costs

The $n = 2$ atom in the full function proves

$$\frac{A_1(-T)}{D_p(-T)} \ge \frac{p^4+1}{16D(4)}e^{(\lambda_2-\lambda_p)T}.$$

At T_+ for $p = 101$, the base-ten logarithm of this lower bound is about 5924. Subtracting independently approximated full functions can therefore amplify relative errors enormously. Evaluating the known positive difference series is a different procedure. These conditioning figures impose no universal precision requirement on every possible recovery algorithm.

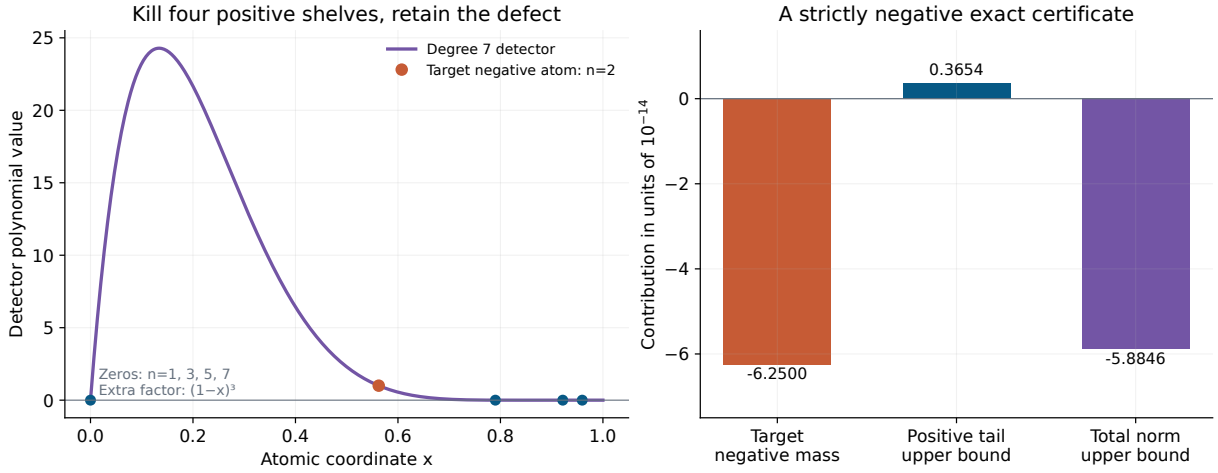
RESOLUTION ATLAS / NEGATIVE ATOMS

A degree-seven witness exposes a signed defect

Let $x_n = (1 - n^{-2})^2$, and change the prime-two sieve strength to $\lambda_2 = -1 - \delta$. For a real polynomial f, the signed quadratic form is

$$Q_\delta(f) = \sum_{\substack{n\geq 1\\ \mu(n)^2=1\\ n \text{ odd}}} \frac{f(x_n)^2}{n^4} - \delta \sum_{\substack{n\geq 1\\ \mu(n)^2=1\\ n \text{ even}}} \frac{f(x_n)^2}{n^4}.$$

Every even squarefree atom has negative mass. At $\delta = 10^{-12}$, the polynomial below certifies that this is detectable at finite degree.



The detector vanishes on the first four positive shelves and equals one at the negative atom $n = 2$. The positive bar is an upper bound for the entire remaining positive tail. The total upper bound is negative, so no omitted atom can reverse the conclusion.

The certificate uses rational arithmetic throughout

Take $S = \{1, 3, 5, 7\}$ and define

$$P(x) = \prod_{n\in S} \frac{x - x_n}{x_2 - x_n} \left(\frac{1 - x}{1 - x_2}\right)^3.$$

Its degree is seven. All remaining positive nodes begin at $n = 11$. With $C = 756482048/20777538825$ and $r = 3856/102487$, a complete tail bound gives

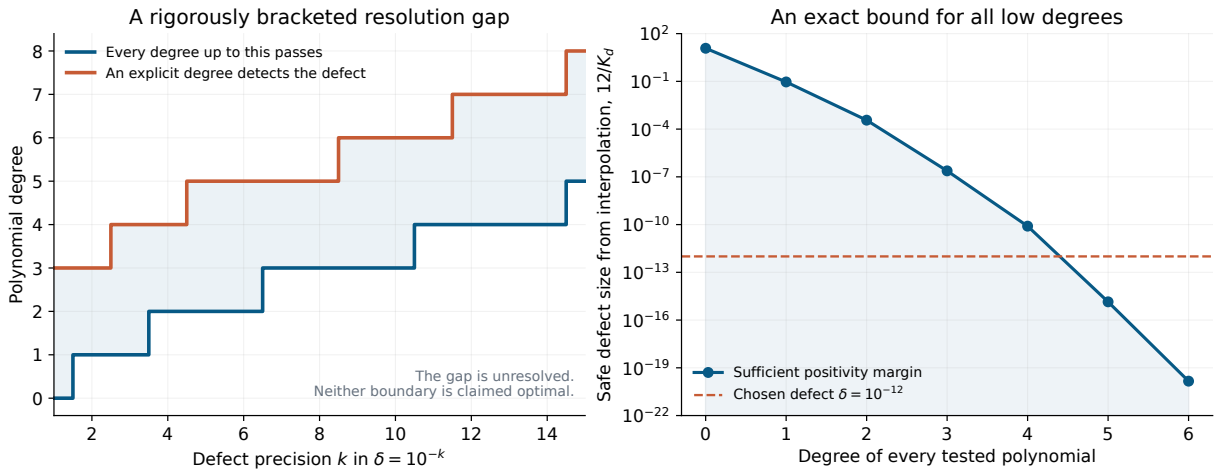
$$Q_{10^{-12}}(P) \leq -\frac{10^{-12}}{16} + \frac{C^2 r^6}{3 \cdot 7^3} < -5.8845708899 \times 10^{-14}.$$

The inequality is certified as a comparison of exact rational numbers. The first four zeros remove the dominant positive contributions. The factor $(1 - x)^3$ suppresses the remaining cluster near one. The construction exhibits a detecting degree, without asserting that degree seven is the smallest possible choice.

RESOLUTION ATLAS / ALL LOW DEGREES

Passing every coarse test can still miss the defect

The previous witness would be less informative without a converse guarantee at lower resolution. For the same defect $\delta = 10^{-12}$, every nonzero polynomial of degree at most four has a strictly positive quadratic-form value. This quantifies the information that the coarse test actually misses.



The blue boundary certifies positivity for every polynomial through that degree. The orange boundary gives an explicit detecting polynomial. The shaded gap remains unresolved by these certificates. At $\delta = 10^{-12}$, degrees through four pass, degree seven fails, and degrees five and six are undecided here.

Interpolation controls the whole polynomial space

Choose the odd squarefree labels $n_i = 1, 3, 5, 7, 11$, write $y_i = x_{n_i}$, and put

$$b_i = \prod_{j \neq i} \frac{\max(y_j, 1 - y_j)}{|y_i - y_j|}, \qquad K_4 = \sum_{i=0}^{4} n_i^4 b_i^2.$$

Lagrange interpolation and weighted Cauchy–Schwarz show that, for every polynomial f of degree at most four,

$$Q_\delta(f) \geq \left(1 - \frac{\delta K_4}{12}\right) \sum_{i=0}^{4} n_i^{-4} f(y_i)^2.$$

Exact rational comparison gives $12/K_4 > 7.9790 \times 10^{-11} > 10^{-12}$. A nonzero polynomial cannot vanish at all five selected nodes, so the right side is strictly positive. Thus the order-five Hankel matrix is positive definite, while the degree-seven witness makes the order-eight matrix fail positive semidefiniteness.

The complete atlas contains the general interpolation and detector bounds. Its reproducible check records 985 exact assertions and 16 floating algebra checks. The proofs establish the universal statements. The tests verify the stated finite certificates and implementations.

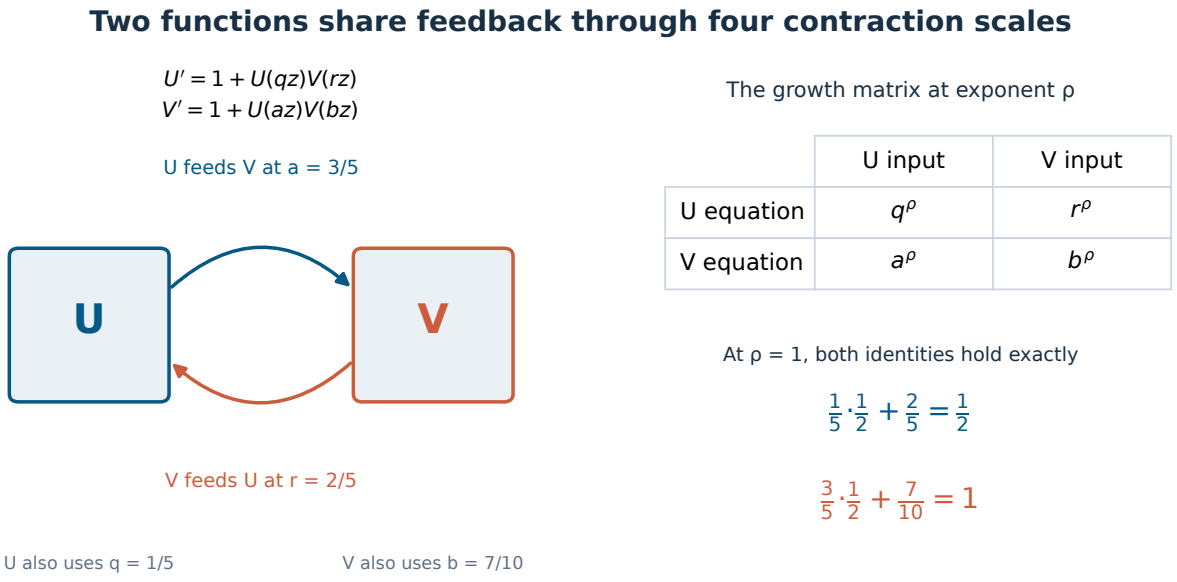
FAMILY 5

Two functions exchange growth

For four real contractions $0 < q, r, a, b < 1$, define the normalized pair

$$\boxed{\begin{aligned} U'(z) &= 1 + U(qz)V(rz), \\ V'(z) &= 1 + U(az)V(bz), \qquad U(0) = V(0) = 0. \end{aligned}}$$

Each equation combines one value of U with one value of V. The four scales specify where that exchange occurs. Both functions begin with the same unit slope, while later coefficients retain the two equations' different scale addresses.



The worked pair $(q, r, a, b) = (1/5, 2/5, 3/5, 7/10)$ has exact order one. The two displayed identities give the positive growth vector $(1/2, 1)^T$.

There is a unique entire solution pair. Both functions are odd, and every odd Taylor coefficient is positive. The common order is governed by the positive matrix

$$P(s) = \begin{pmatrix} q^s & r^s \\ a^s & b^s \end{pmatrix}, \qquad \operatorname{spr} P(\rho) = 1.$$

The eigenvector supplies the relative weights that a row sum misses. In the example, the row sums at $s = 1$ are $3/5$ and $13/10$. The coupled system nevertheless has order exactly one in both components.

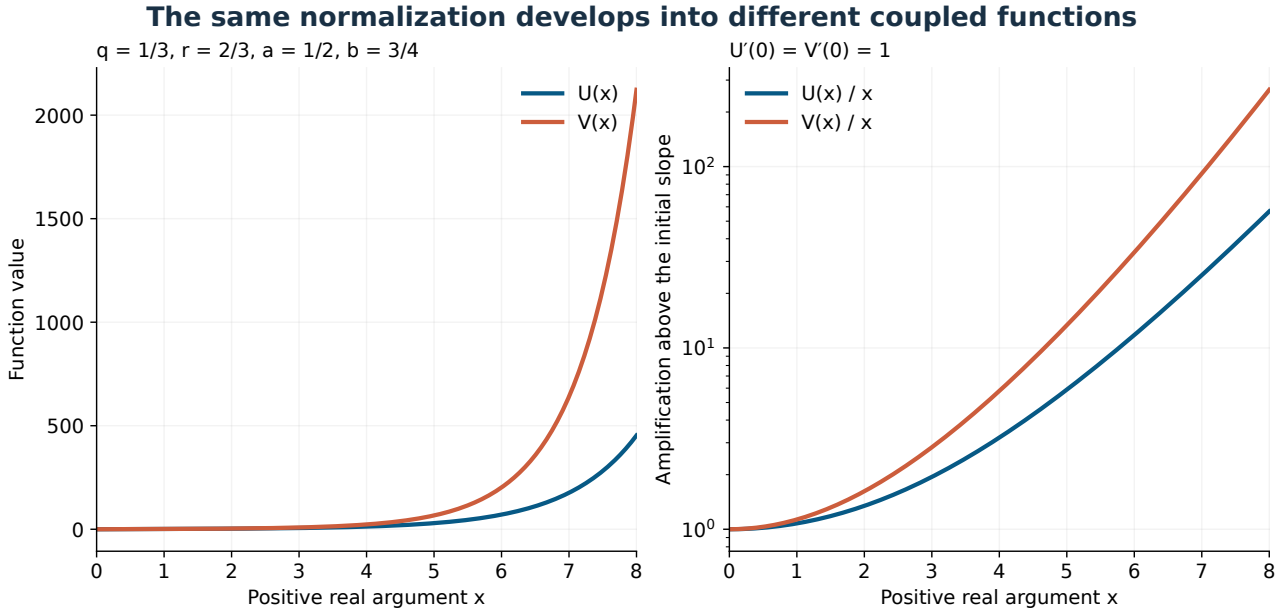
FAMILY 5 / CONSTRUCTION

The coefficients preserve both addresses

Write $U(z) = \sum_{n\geq 0} u_n z^{2n+1}$ and $V(z) = \sum_{n\geq 0} v_n z^{2n+1}$, with $u_0 = v_0 = 1$. The first equation gives the exact recursion

$$u_n = \frac{1}{2n+1} \sum_{i+j=n-1} q^{2i+1} r^{2j+1} u_i v_j, \qquad n \geq 1.$$

The second replaces (q, r) by (a, b) while retaining the same products $u_i v_j$. Thus each new coefficient uses the shared history of the pair.



For $(q, r, a, b) = (1/3, 2/3, 1/2, 3/4)$, the components separate despite their common initial slope. These numerical curves use odd indices through 240. The two truncations at indices 120 and 240 agree at $x = 8$ to displayed double precision.

The first distinction already appears at degree three:

$$U(z) = z + \frac{qr}{3} z^3 + O(z^5), \qquad V(z) = z + \frac{ab}{3} z^3 + O(z^5).$$

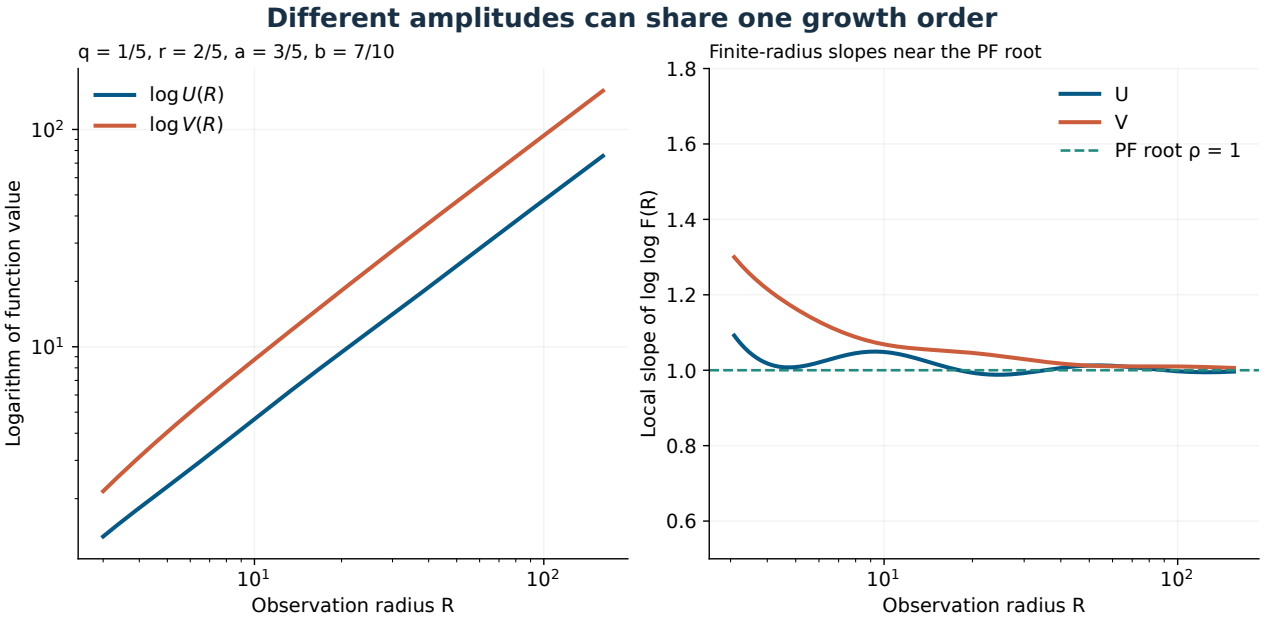
Induction gives $0 < u_n, v_n \leq 2^{-n}$, which supplies a convergent germ. If both functions are known on a disk of radius R, their integral equations extend them to radius R/Q, where $Q = \max(q, r, a, b) < 1$. Repeating this step reaches every finite disk.

The numerical agreement above checks the plotted approximation. The later certificate page supplies an exact bound on the omitted tail.

FAMILY 5 / GROWTH

One order, two exact type proportions

The entire functions have the same order ρ, with positive lower type and finite upper type. Positivity places the maximum modulus on the positive real axis, so $M_U(R) = U(R)$ and $M_V(R) = V(R)$.



The order-one example has different component amplitudes. The right panel shows finite-radius slopes near one. The curves use odd indices through 800. Agreement with index 400 is a numerical diagnostic, and the order itself follows from the analytic proof.

For $F_1 = U$ and $F_2 = V$, define

$$\underline{\tau}_i = \liminf_{R\to\infty} \frac{\log M_{F_i}(R)}{R^\rho}, \qquad \overline{\tau}_i = \limsup_{R\to\infty} \frac{\log M_{F_i}(R)}{R^\rho}.$$

If $P(\rho)w = w$ with $w > 0$, then both type vectors have precisely these Perron proportions:

$$\boxed{\underline{\boldsymbol{\tau}} = \underline{\tau}\, w, \qquad \overline{\boldsymbol{\tau}} = \overline{\tau}\, w, \qquad 0 < \underline{\tau} \le \overline{\tau} < \infty.}$$

For the worked pair, both the lower type and the upper type of V are twice the corresponding type of U. Either both ordinary type limits exist or neither does. Equality of the lower and upper types remains open. The finite-radius slope picture does not decide that question.

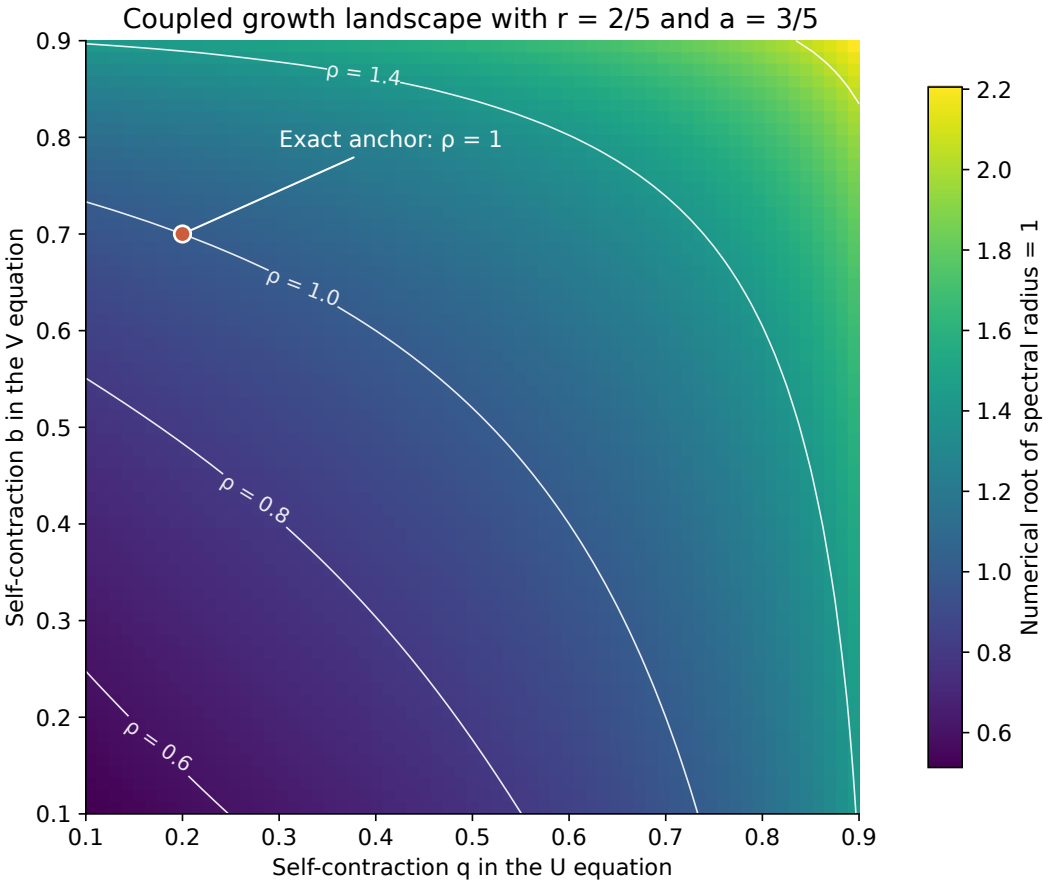
FAMILY 5 / PARAMETER SPACE

Growth follows a spectral surface

The order is the unique positive solution of

$$\boxed{(1-q^\rho)(1-b^\rho)=(ar)^\rho.}$$

The left side increases from zero to one as ρ increases. The right side decreases from one to zero. Their unique crossing determines the growth exponent without fitting a truncated Taylor curve.



Numerical solutions of the proved characteristic equation, with $r=2/5$ and $a=3/5$. The highlighted pair $(q,b)=(1/5,7/10)$ has order exactly one by rational arithmetic.

The order depends on the self scales q,b and on the product ar of the cross scales. Holding q,b,ar fixed preserves the order, while changing the cross scales separately generally changes the functions and their type proportions:

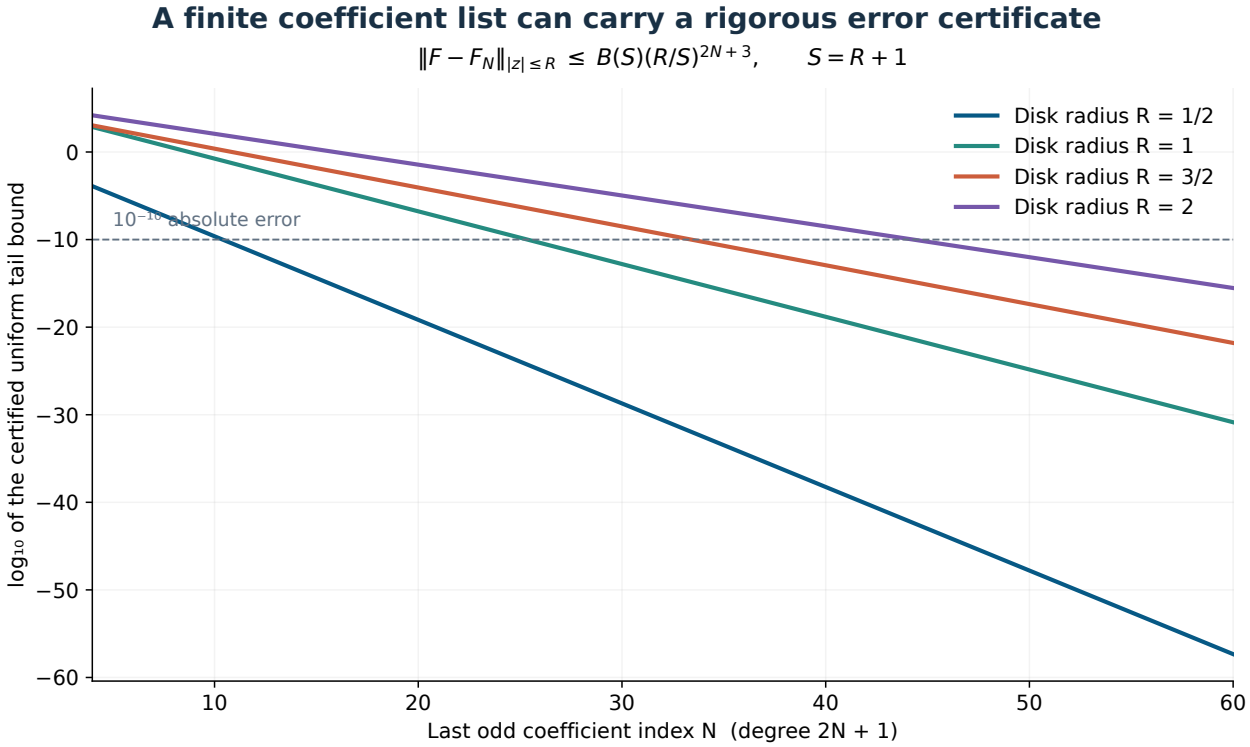
$$\frac{w_1}{w_2}=\frac{r^\rho}{1-q^\rho}=\frac{1-b^\rho}{a^\rho}.$$

Consequently, equal order does not determine the family member. It fixes one growth exponent within a larger parameter space. The coefficients carry enough additional information to recover all four ordered scales away from the reduction surfaces described below.

FAMILY 5 / PRECISION

A coefficient list with a certified tail

A finite Taylor list becomes an exact approximation certificate when it is paired with a bound on a larger disk. Let F be either component, and let F_N retain the odd indices $0, \dots, N$.



Each curve is computed from an exact rational upper bound for the same worked pair. Increasing the coefficient count certifies a smaller uniform error on the stated complex disk. The logarithmic plotting coordinates are rounded.

Put $Q = \max(q, r, a, b)$. One elementary majorant starts with $B(x) = x/(1 - x^2)$ for $0 \le x < 1$ and works outward through the finite contraction ladder using

$$B(x) = x\big(1 + B(Qx)^2\big).$$

The integral equations show that this bounds both components on the disk $|z| \le x$. For $S > R \ge 0$, positivity then gives

$$\max_{|z| \le R} |F(z) - F_N(z)| \le B(S) \left(\frac{R}{S}\right)^{2N+3}.$$

The exponent is the first omitted odd degree. Every later term has an even smaller ratio between its values at radii R and S. For the worked pair, $N = 30$, $R = 1$ and $S = 2$ give an error below 1.600×10^{-13} for both functions. The laboratory returns rational interval endpoints, so the certificate survives decimal rounding.

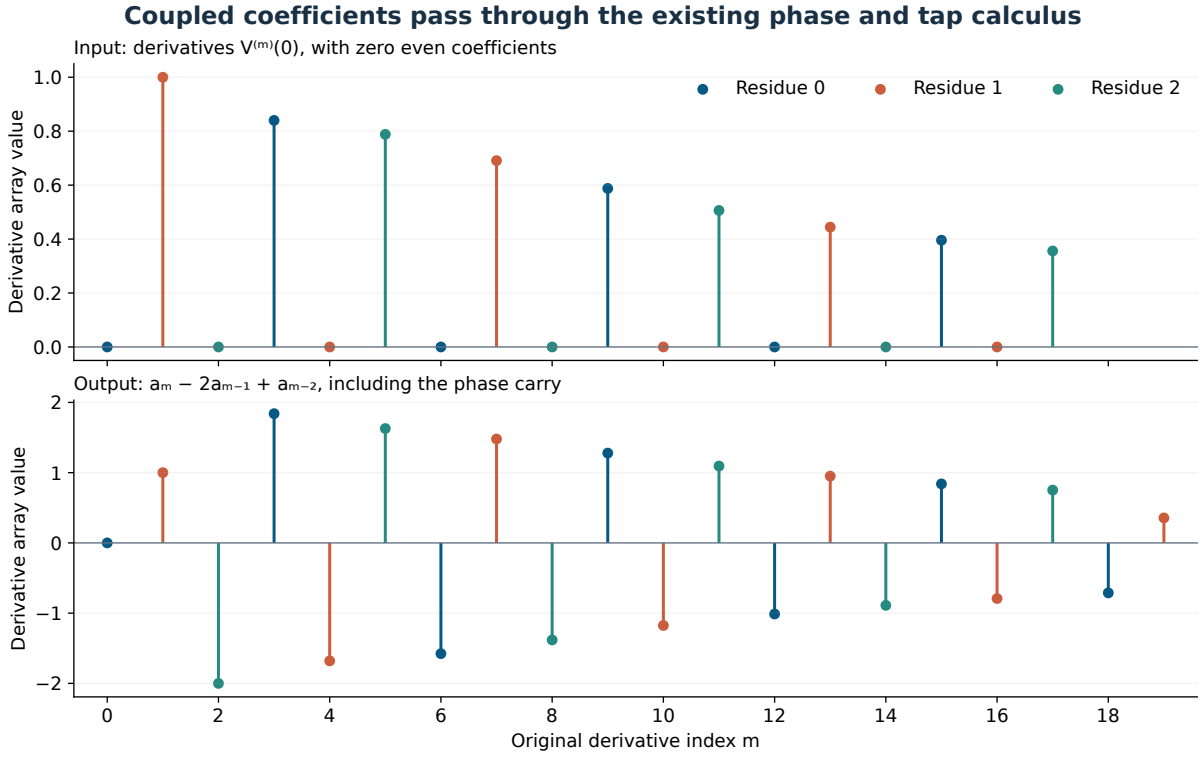
FAMILY 5 / SEQUENCES

The phase calculus transports the pair

Use the derivative normalization $A_n = (2n+1)!u_n$, $B_n = (2n+1)!v_n$. Its recurrence has integer binomial weights:

$$A_n = \sum_{i+j=n-1} \binom{2n}{2i+1} q^{2i+1} r^{2j+1} A_i B_j, \qquad n \geq 1.$$

The second component again replaces (q, r) by (a, b).



The full derivative array of V is split into three residue lanes. Applying taps $(1, -2, 1)$ with the correct block carries, then interleaving, agrees exactly with direct convolution.

These derivative arrays are polynomials with nonnegative integer coefficients in the four scale variables. Their total degree is at most $n(n+1)$. If every parameter denominator divides D_0, then

$$D_0^{n(n+1)} A_n, \qquad D_0^{n(n+1)} B_n \quad \text{are integers.}$$

This uniform clearing factor makes exact rational families available to integer sequence experiments. It need not be the smallest possible factor.

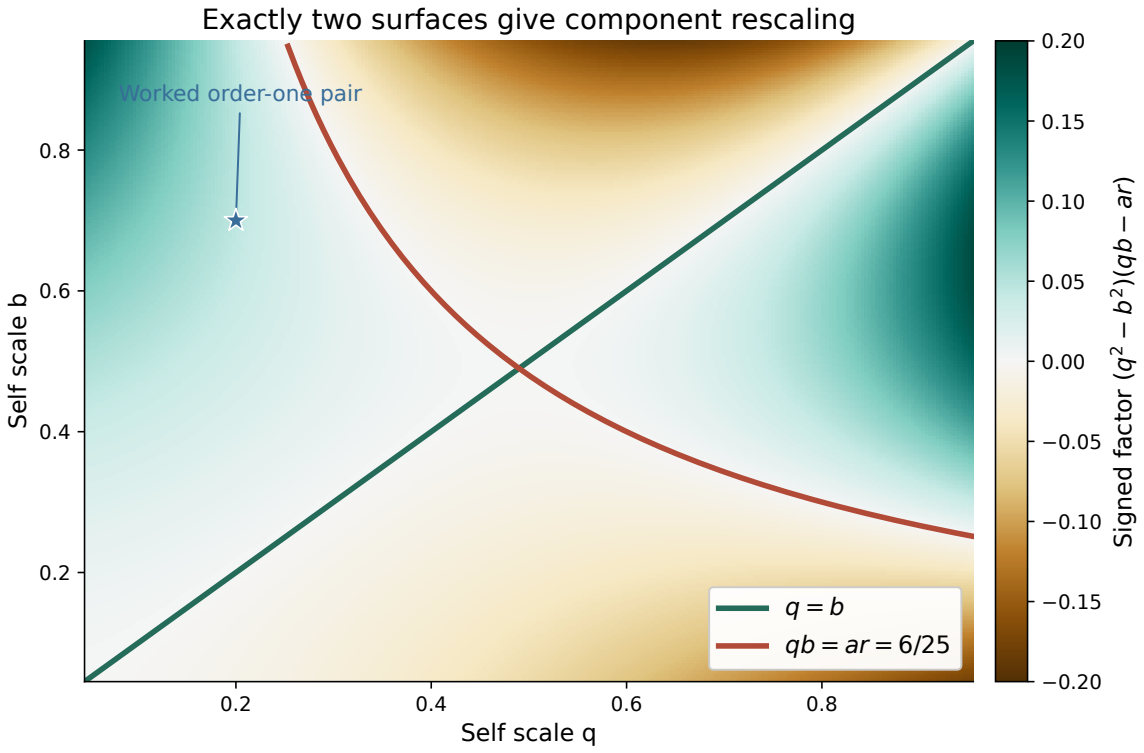
Ordinary taps on a derivative array correspond to repeated integration shifts of its exponential generating function. Multiplication of two exponential generating functions instead requires binomial convolution. The catalog preserves that distinction and marks generic integer and signed scale examples as formal series outside the proved analytic domain.

FAMILY 5 / REDUCTION

Two surfaces where one component rescales to the other

Set $p = qr$, $k = ab$, and use the ordinary Taylor coefficients u_2, v_2 at degree five. The exact separation quantity factors as

$$D = k^2 u_2 - p^2 v_2 = \frac{pkar}{15}(q^2 - b^2)(qb - ar).$$



The two reduction surfaces are $q = b$ and $qb = ar$. Their union is exactly the zero set of D in the positive contraction domain. Outside this union, the components cannot be obtained from each other by amplitude and argument rescaling.

There exist nonzero complex constants A, B with $V(z) = A\,U(Bz)$ if and only if $D = 0$. On either surface, put $s = \sqrt{k/p} > 0$. The scalar family is defined by $T'_{x,y}(z) = 1 + T_{x,y}(xz)T_{x,y}(yz)$, $T_{x,y}(0) = 0$. It gives the explicit reduction

$$U(z) = \sqrt{s}\,T_{q,sr}(z/\sqrt{s}), \qquad V(z) = s^{-1/2}T_{q,sr}(\sqrt{s}\,z).$$

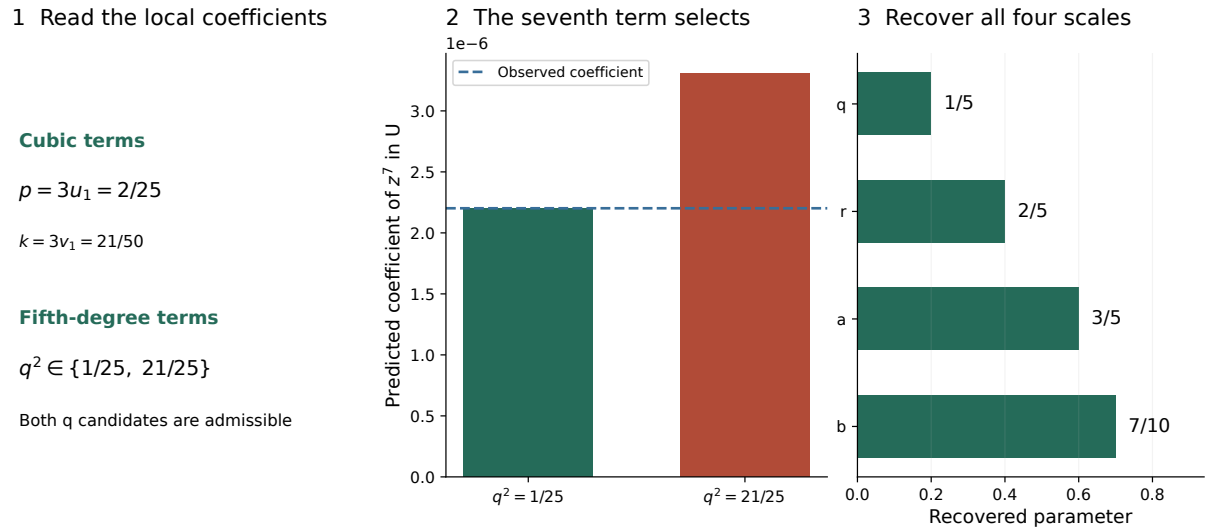
Both effective scales lie in $(0, 1)$. Equality $U = V$ is more restrictive: it occurs exactly when $\{q, r\} = \{a, b\}$.

This classifies relations between the normalized components. Separately, no invertible constant linear coordinate change decouples the defining operator into two autonomous scalar equations on every analytic input. That operator statement does not exclude nonlinear changes of variables or other special-function identities.

FAMILY 5 / RECOVERY

Degree seven identifies the four scales

Away from $D = 0$, the six coefficients $(u_1, v_1, u_2, v_2, u_3, v_3)$ uniquely recover the ordered parameters (q, r, a, b) in $(0, 1)^4$. These are the coefficients at degrees three, five and seven of the two labeled functions.



Cubic terms recover the two scale products. Fifth-degree terms leave at most two candidates for each remaining scale. The seventh-degree terms select the unique admissible candidates when $D \neq 0$. Repeated quadratic roots are already unique.

First $p = 3u_1$ and $k = 3v_1$. The possible values $x = q^2$ and $y = a^2$ satisfy

$$px^2 - \frac{15u_2}{p}x + kp^2 = 0, \qquad py^2 - \frac{15v_2}{k}y + k^3 = 0.$$

For two distinct positive candidates x, x', the predicted seventh coefficients differ by

$$u_3(x) - u_3(x') = \frac{pD}{7k^2}(x^2 - x'^2) \neq 0.$$

The second component supplies the analogous separation for y. Finally take the positive square roots and recover $r = p/q$, $b = k/a$.

This is an exact-data inverse theorem. Near a reduction surface, small D can make candidate predictions close, so a uniform stable inverse does not follow. The degree-seven recovery and the reduction classification are proved statements. Historical priority of these particular results is addressed separately by the bounded literature comparison.

EVIDENCE / COUPLED FAMILY

What the coupled extension establishes

Result	Scope
Coupled entire construction	Unique normalized pair for four positive strict contractions, with positive odd coefficients
Common growth law	Exact order from the characteristic matrix, positive lower type, finite upper type, and exact Perron proportions for both type vectors
Component reduction	Rescaling occurs exactly on $q = b$ or $qb = ar$
Generic exact inverse	Coefficients through degree seven identify all four ordered scales when $D \neq 0$
Operator obstruction	No invertible constant linear change decouples the defining operator on all analytic inputs
Resolution certificates	Explicit compact, radius, prime-depth and polynomial-degree bounds for the three worked examples

Verification and reproducibility

The coupled-system finite suite passes **5,272 exact assertions and 26 numerical assertions**. Thirteen input and resource guards are recorded separately. The exact inverse is checked on 256 rational parameter tuples. The coupled API is compared with an independent dense Picard construction and classical anchors. The resolution checks verify the exact rational certificates. These counts are separate from the earlier four-family evidence of 19,871 exact and 5,576 numerical assertions.

The project's recorded mathematical review reconstructs the proof implications and checks the preserved source files. This record is not external peer review. It corrected an initial-segment quantifier in the detector theorem. The worked certificate already used that initial segment. The source package records the correction, the repair of a figure label, and the successful checks.

Questions that remain open

The coupled theorem does not determine an ordinary type limit, uniform angular growth, or the complex zero geometry. Stable finite-precision recovery near the reduction surfaces remains open. The resolution bounds are constructive and can be conservative. The sieve example leaves degrees five and six undecided. The literature comparison does not settle historical priority.

The exact API and its checks run with the Python standard library. NumPy, Matplotlib, and mpmath generate the figures. The full manuscript supplies the proof appendices and the source archive contains the code and inputs needed for the computations.

REFERENCES / RELATED SYSTEMS

Where the coupled construction sits

The entire-order and type results are proved directly in this edition. The surrounding mechanisms have classical antecedents, whose precise relationship is recorded in the included literature comparison.

Miguel A. Méndez, 2024. *Combinatorial differential operators in: Faà di Bruno formula, enumeration of ballot paths, enriched rooted trees and increasing rooted trees*, Australasian Journal of Combinatorics 89(3), 350–384. Theorem 2.1 and Example 2.4 give the scalar diagonal equation. https://ajc.maths.uq.edu.au/pdf/89/ajc_v89_p350.pdf

H. Alrabaiah, I. Ahmad, K. Shah and G. Ur Rahman, 2020. *Qualitative analysis of nonlinear coupled pantograph differential equations of fractional order with integral boundary conditions*, Boundary Value Problems, article 138. Its coupled fractional boundary-value system is an adjacent construction with different hypotheses and conclusions. https://doi.org/10.1186/s13661-020-01432-2

Pawel Blasiak and Philippe Flajolet, 2011. *Combinatorial Models of Creation–Annihilation*, Séminaire Lotharingien de Combinatoire 65, B65c. Proposition 24 and Note 25 describe multitype increasing trees and differential systems. https://arxiv.org/abs/1010.0354v3

R. Daniel Mauldin and S. C. Williams, 1988. *Hausdorff Dimension in Graph Directed Constructions*, Transactions of the American Mathematical Society 309(2), 811–829. Theorems 2 and 3 use a spectral-radius equation for a geometric dimension. Here the same form of spectral balance determines an analytic growth order through a separate proof. https://sites.math.unt.edu/~mauldin/papers/no67.pdf

Radu Dascaliuc, Tuan N. Pham, Enrique Thomann and Edward C. Waymire. *Transformation of Stochastic Recursions and Critical Phenomena in the Analysis of the Aldous-Shields-Athreya Cascade and Related Mean Flow Equations*, arXiv:2411.00629v2. Equation (1.8) is an adjacent nonlinear Riccati delay model. https://arxiv.org/abs/2411.00629v2

Charles Knessl and Wojciech Szpankowski, 2006. *Binary Trees, Left and Right Paths, WKB Expansions, and Painlevé Transcendents*, ANALCO, 198–204. Its ordinary generating function satisfies $C(z) = 1 + zC(wz)C(vz)$, a related dilation-product identity with different normalization and coefficient rules. https://www.cs.purdue.edu/homes/spa/papers/analco06.pdf

This is a bounded comparison rather than an exhaustive historical survey. The complete record contains exact locators, inspected statements, terminology variants and search limits. It leaves priority unresolved for the particular results of this edition.